IEEE Access
Multidisciplinary | Rapid Review | Open Access Journal

Received 24 May 2023, accepted 17 June 2023, date of publication 26 June 2023, date of current version 6 July 2023.

Digital Object Identifier 10.1109/ACCESS.2023.3289301

RESEARCH ARTICLE

Field Distribution Features of Linearly Polarized Field of Plane Aperture

SERGEY P. SKULKIN[1], GRIGORY K. USKOV[2], (Member, IEEE), NIKOLAY A. LYSENKO[2], AND NIKOLAY I. KASCHEEV[1]

[1]Department of the MERA Group of Companies, National Research University Higher School of Economics, 603093 Nizhny Novgorod, Russia
[2]Department of Electronics, Voronezh State University, 394018 Voronezh, Russia

Corresponding author: Sergey P. Skulkin (ssp132@mail.ru)

This work was prepared as a result of research (project no 22-00-035) within the framework of the Scientific Foundation Program of the National Research University Higher School of Economics (HSE).

ABSTRACT In this study, we describe the specific features of the near-field distribution of a uniformly illuminated aperture. An analytical method based on physical optics in the time domain is used to calculate the field intensity. The primitive impulse response function makes it possible to calculate the near-field distribution of the antenna. The difference in the amplitudes of the fields during the observation point shift along the X and Y coordinate axes can reach up to 13% of their maximum relative values. This difference should be considered when calculating the antenna radiation patterns. At the end of this paper, we present the results of the comparison obtained using three methods: geometrical theory of diffraction (GTD), plane wave spectrum approach (PWS), and primitive impulse response function (IRF) method. In the near field of relatively small apertures (with respect to wavelength), the results of all three compared methods (GTD, PWS, and IRF) were very similar. The analytical IRF method, the results of which are given in this paper, is much more effective in terms of computer resources than the plane wave spectrum approach, and even more effective than the geometric theory of diffraction method.

INDEX TERMS Near field analysis, physical optics, aperture antennas, spatial-frequency characteristics, ultra-wideband antennas.

I. INTRODUCTION

The problem of the near-field distribution of a uniformly illuminated aperture was discussed 50–70 years ago [1], [2], [3], [4], [5], [6], [7]. It has already been shown that the plane wave spectrum (PWS) formulation [2], [3], [4] has several advantages over the aperture integration approach for calculating the near field of circular apertures. The PWS approach has also been found to be useful for determining the far-field directivity patterns of large antennas using near-field measurements [4], [5] and further recalculations. In [1], new expressions were given, which are extremely effective for near-field calculations because they are expressed as Fresnel integrals or elementary functions. PWS method calculations are more efficient than the geometric theory of diffraction (GTD) method.

The GTD method [8], [9], [10], [11], [12], [13] was first described by Keller in 1962 [8]. The accuracy analysis of the PWS and GTD [6] yielded similar results for a homogeneous slit and circular hole. In [6] it was concluded that the PWS method is essentially a near-field method, whereas the GTD method is generally a far-field method. After a long discussion of the results obtained by both methods, figures showing close or identical results for both methods are provided [6].

An analytical method for physical optics in the time domain to calculate the field was proposed in [14], [15], [16], [17], and [18]. In [14], the time dependence of the field, which is the primitive of the impulse response function (PIRF) of the aperture and propagation media at any point in the front

The associate editor coordinating the review of this manuscript and approving it for publication was Pavlos I. Lazaridis.

half space of the aperture, was calculated. Aperture theory approximation was used, which considers each aperture point to emit a δ pulse.

A new analytical approach based on physical optics in the time domain for the PIRF of a circular aperture in the form of a second-kind elliptic integral and its features were presented in [15] and [16]. In these papers, it was clearly shown that a linearly polarized field (i.e., along the Y-axis) in front of the antenna aperture differs with parallel (Y) and perpendicular (X) offsets of the observation point.

In [16], it was argued that compared with the use of other well-known methods for calculating monochromatic fields (i.e., plane-wave spectrum theory, physical optics, or Kirchhoff formulation), the PIRF calculation method often allows obtaining more accurate values for the spectral components of the field [18]. This is because the accuracy of calculating the spectral components is determined by the accuracy of the field representation and one-dimensional Fourier transform procedure (by choosing a time window and sampling step).

The obtained analytical results were verified by the Finite Integration Technique (FIT) numerical calculation in [16]. The comparison of analytical (Impulse Response Function) and numerical (Finite Integration Technique) results yielded a good agreement for all frequencies less than the boundary, distances and offsets [16]. Also, the authors showed there the advantage of the analytical approach in terms of computational time and/or resources. Using the IRF method, one can find the monochromatic field distribution much faster than numerically reaching a similar accuracy.

This paper presents a method for calculating a monochromatic field, obtained as a Fourier transform of its time dependence, based on the PIRF approach (previously called the PRC method) [14].

The purpose of this paper is to analyze and explain the behavior of the field while observing point shifts along the X, perpendicular to, and Y, parallel to the polarization, when an aperture is excited by a linearly polarized plane wave. An EM field is formed by short-pulse radiation from the aperture. Such a "fine" field structure helps to explain the physics of the process and shows the possibilities of the method for calculating the fields.

In addition, we consider how the electromagnetic field of the ultra-wideband pulse affects the monochromatic near-field.

We compared the results of this PIRF method with those given in [6], obtained by the GTD and PWS methods at a short distance from the aperture. The comparison shows the complete correspondence of all results obtained by the three methods.

We also present the results of a comparison of the PIRF method with PWS for an observation point at a distance from the aperture plane z = 1000λ, with an aperture diameter D = 1000λ. We observed insignificant discrepancies in some of the plots. A discussion of the results is also provided.

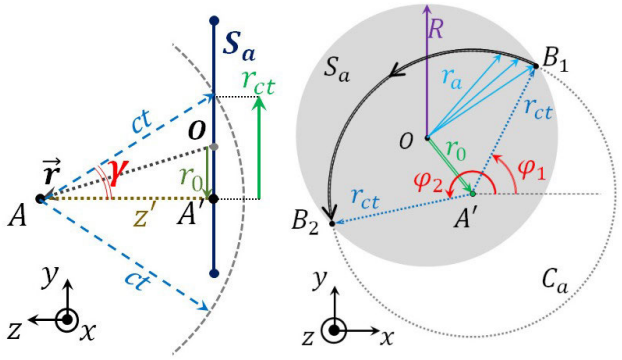

FIGURE 1. Geometry of the problem.

II. TIME DOMAIN ANALYSIS

The details of the geometry are shown in Fig. 1a,b. At each time moment t the integration angles ϕ_1 and ϕ_2 (see Fig.1b) along a part of the circle C_a are determined by the points B_1, B_2 where this contour intersects with the border of the aperture S_a. γ is the angle between $\vec{r}$ and perpendicular to the aperture plane (see Fig. 1a). The limits of integration ϕ_1, ϕ_2 depend on the position of the observation point $\vec{r}$ in such a way that both values can vary from zero to 2π. R is the radius of the circular aperture, the contour C_a is a circle with radius $\vec{r_{ct}}$ centered at point A' – the projection of A, $\vec{r_0}$ is the projection of the $\vec{r}$, $\vec{r_a}$ is the vector up to the set of points on the aperture over which the integration is carried out. The axes OX, OY and OZ are shown in the lower left corners of Figures 1a,b.

In [13], a new expression for the polarization multiplier and electromagnetic field strength at an arbitrary point in front of the aperture was derived:

$$\hat{E}(\vec{r}, t) = \frac{1}{2\pi} \int_{\varphi_1}^{\varphi_2} \sqrt{1 - k^2 \sin^2(\varphi)} d\varphi = \frac{1}{2\pi} \mathbb{E}\left(\varphi \,|\, k^2\right). \tag{1}$$

Here, PIRF $\hat{E}(\vec{r}, t)$ at an arbitrary point $\vec{r}$ can be found as $\mathbb{E}\left(\varphi \,|\, k^2\right)$ – an elliptic integral of the second kind with parameter $k = \sin(\gamma)$, where γ is the angle between the radius vector and point $\vec{r}$ and is perpendicular to the aperture plane (see Fig. 1a). This is an analytical integral without a precise value, and cannot be expressed in terms of elementary or polynomial functions.

We define the impulse response function, $h(\vec{r}, t)$ as:

$$h(\vec{r}, t) = \partial \hat{E}(\vec{r}, t) / \partial t \tag{2}$$

This expression describes the impulse response function (IRF) $h(\vec{r}, t)$ and represents the impulse response of the medium between an aperture and an arbitrary point $\vec{r}$, which is considered to be a receiver (or observer).

Fig. 2 shows the PIRFs calculated for the antenna with $D = 1$m at a distance from the circular aperture $z = 0.5R$ for different offsets from the central axis $r_0 = 0.5R, 1R, 1.5R$

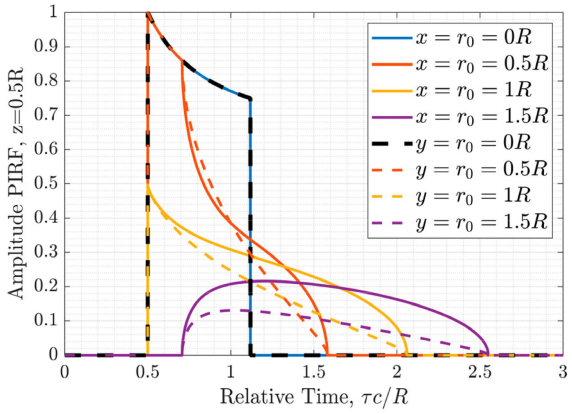

FIGURE 2. PIRF for different point offsets along the X or Y coordinate from the central axis.

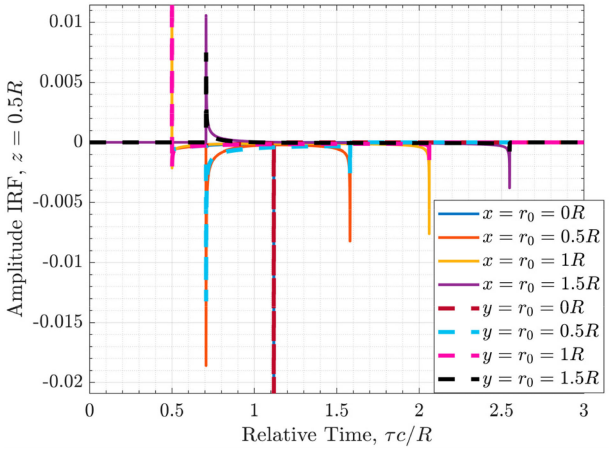

FIGURE 3. Derivative of the PIRF (IRF) for different offsets along the X or Y coordinate from the central axis.

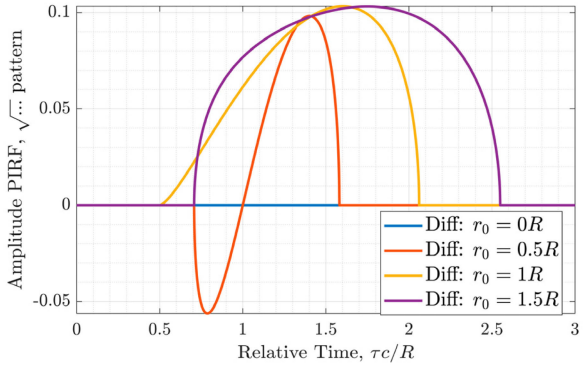

FIGURE 4. Difference between PIRFs with the same offset along X and Y.

in two directions along the X- and Y-axes. For $r_0 = 0R$ the PIRFs and IRFs are the same, whereas for other offsets, they have different shapes and pulse trailing edges, which is the result of the behavior of the polarization multiplier $\alpha(\vec{r}, \vec{r}_a) = \sqrt{1 - k^2 \sin^2(\varphi)}$, which describes the EM field behavior at different polarizations [13].

To obtain these figures, we use the expression from [15], which implies that the aperture consists of an infinite number of infinitesimal dipoles, and each of them has an antenna pattern in the form of a circular torus similar to a vertical infinitesimal dipole. As the observation point shifts inside the projector beam (the distance from the central axis is less than the aperture radius) toward the edge of the aperture, the duration of the PIRF trailing edge increases (Fig. 2, 3 and 4). Simultaneously, the PIRF fronts have the same start-end position in time, which is determined by the geometric dimensions of the aperture and the position of observation point $\vec{r}$.

However, the PIRF curve depends not only on the point displacement relative to the aperture axis but also on the polarization multiplier. As soon as we study the field-intensity dependence on the offset along the axes, the observation point here indicates an infinitely small dipole with the center at that point. When there is an offset along the X-axis, the second edge of the PIRF is higher (Fig. 2 and 4) and thus has a higher first-time derivative (Fig. 3, 5). As offset r_0 shifts inside the projector beam, the duration of the distance between edges increases owing to the trailing edge; as offset r_0 goes outside the projector beam, both the forward and trailing edges change and the amplitude drops (see Fig. 2).

Fig. 3 shows the derivatives of PIRF for the same point shifts along X and Y, as shown in Fig. 2. As it can be seen, the IRF is represented by the same first pulse inside the projector beam and changing second pulse. At the same observation point displacement, although with different shifts along the X- and Y-axes, the appearance of the second pulse was different. The same r_0 offset simultaneously yielded negative pulses at the same time. The IRF at the point along the X-axis has a larger amplitude of the second pulse than that when oriented along the Y-axis because the infinitesimal dipole is oriented vertically.

Fig. 4 shows the difference between PIRFs with the same X- and Y-axis offsets, as shown in Fig. 2. In this figure, the difference reached a maximum at a relative time closer to the end of the PIRF. This confirms that the inequality is caused by the boundary wave [16].

The maximum absolute value of this difference is approximately 0.11 of the full PIRF amplitude. In [16], two wavefronts from the aperture were described: the main wave and the boundary wave. In fact, a maximum relative difference of ≈ 0.13 is observed in the immediate vicinity of the aperture when the distance $z \to 0$, but we consider the field at distance $z = 0.5R$. Half-aperture distances are commonly used for near-field, short-focus reflector antenna measurements.

The difference observed for a boundary wave is shown in Fig. 4, which shows the difference that appears because of the non-uniformity of the field distribution and also helps to prove that the maximum absolute value of this difference is independent of the offset r_0 from the central axis. In Fig. 5 the derivatives of the curves shown in Fig. 4 are plotted.

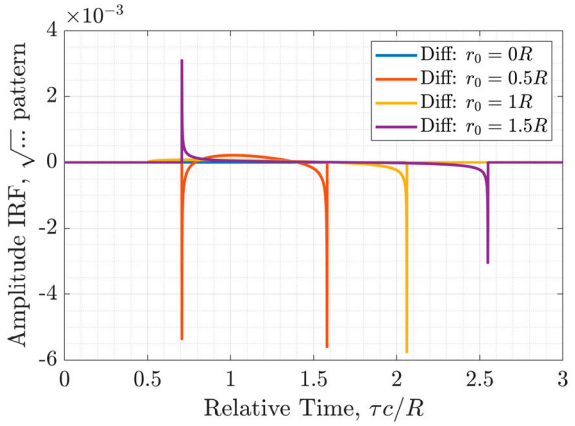

FIGURE 5. Derivative of curves shown in Fig. 4.

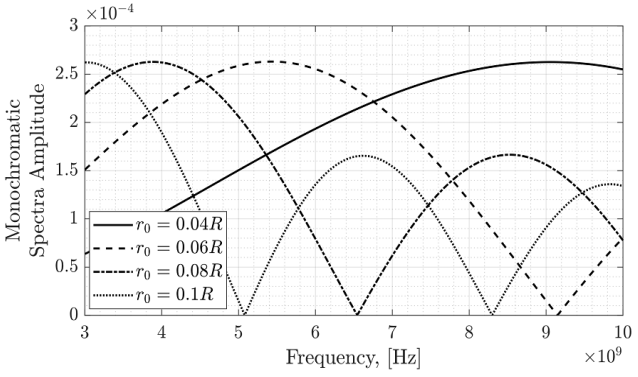

FIGURE 6. Several spectra of PIRF differences (i.e. on Fig. 4) at small offsets, r_0, from the central axis.

The curves presented in Fig. 4 are frequency dependent, and their spectra are shown in Fig. 6. Here we assume that the antenna can be called "an aperture antenna" only if $D/\lambda \geq 10$, that for $R = 0.5m$ means $f \geq 3$ GHz. From this figure, we can see that the maximum value of the spectrum amplitude remained the same at approximately $2.6 \cdot 10^{-4}$ across small offsets r_0. At larger r_0 the maximum value decreases. This means that we can investigate the field behavior at 3-9 GHz, by saying that at other higher frequencies, the field difference between the X and Y point offsets of the point would be lower.

The field behavior with respect to offset r_0 can be explained as follows. Two wavefronts existed inside the projected beam [16]. At the central axis, a wavefront from the boundary interferes with itself, thus yielding a higher amplitude. At r_0 equal to half the aperture distance, the wavefront from the opposite boundary arrives at a different time, so no constructive interference is observed.

III. FREQUENCY DOMAIN ANALYSIS

The Fourier transform of the IRF $h(\vec{r}, t)$, assuming $f = c/\lambda$, gives us the so-called space-frequency response of the system

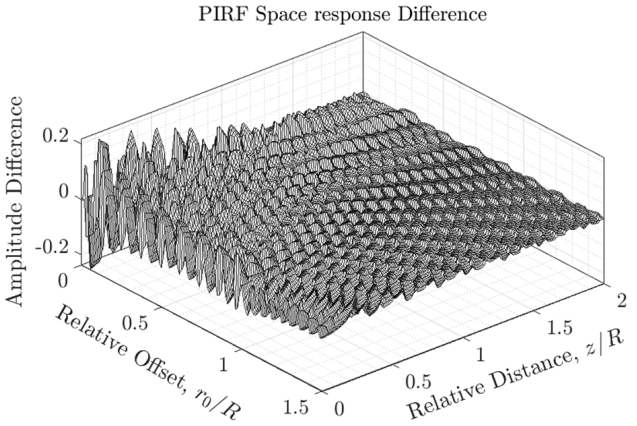

FIGURE 7. Absolute difference between the fields along the X- and Y-axes in the near-field space for $R = 0.5$m and $F = 5$ GHz. ($\lambda = 0.06$ m) as a function of the relative distance from the aperture and from the center.

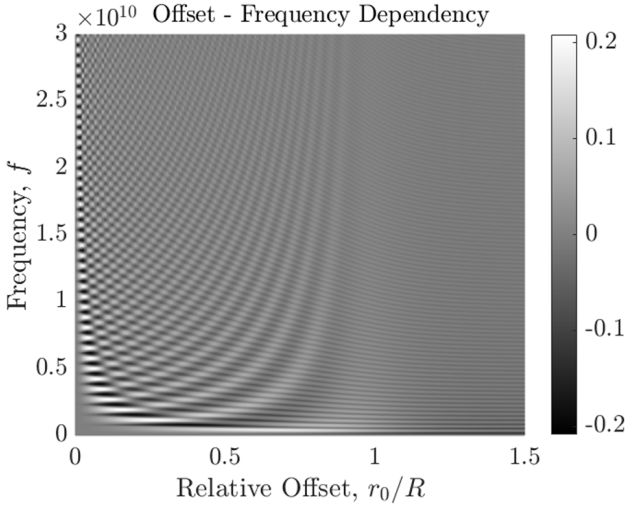

FIGURE 8. The absolute difference between the fields for R = 0.5m, z = 0.5R depending on frequency and relative offset itself r_0.

"aperture + free space to the point" $K^*(\vec{r}, f)$:

$$h^*(\vec{r}, f) = K^*(\vec{r}, f) = \int \frac{\partial \hat{E}(\vec{r}, t)}{\partial t} e^{j2\pi ft} dt \qquad (3)$$

Fig. 7 shows the absolute difference between the fields along the X- and Y-axes in the near-field space for $R = 0.5$ m and $f = 5$ GHz ($\lambda = 0.06$ m) as a function of the distance from the aperture. As can be seen from the figure, the difference has extremums near the Z-axis of the aperture but has a zero value on the axis itself. This effect was observed because $r_0 = 0$ indicates a zero offset along the X-and Y-axis.

The absolute difference between the fields in the near-field space for $R = 0.5m$, $z = 0.5R$ depending on frequency and relative offset is represented in Fig. 8 (it is generalization of the Fig. 6). The main idea of this figure is to capture and show, first, the difference in the field intensity for a given frequency along offset r_0z, and second, the variation of the fiel for a chosen offset r_0 across different frequencies. There

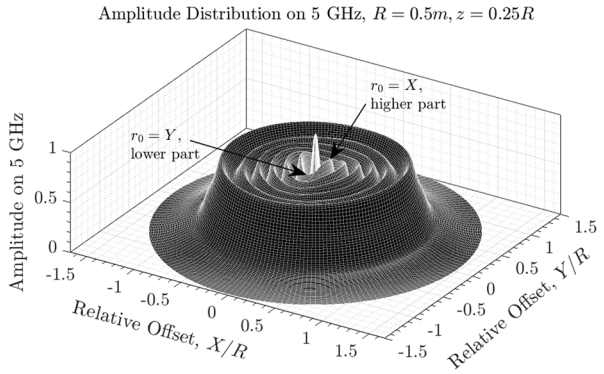

FIGURE 9. The volumetric field distribution over the aperture for distance z = 0.25R, f = 5 GHz.

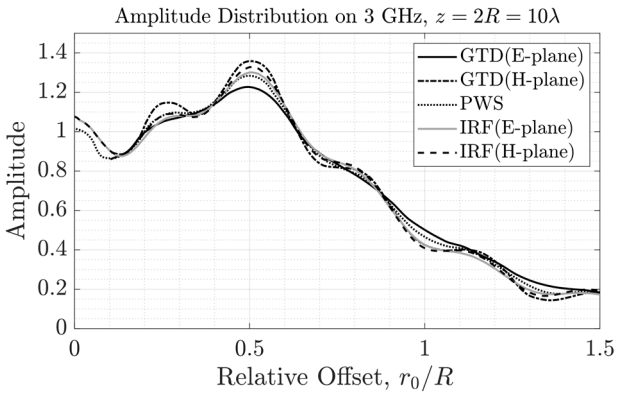

FIGURE 10. The near-field calculation results for a circular aperture. Distance to the aperture plane z = 10λ (diameter D = 10 λ).

is a vague boundary seen for $r_0/R = 1$ between the projector beam with "waves" and the other half-space. In addition, this three-dimensional surface can be used as a reference for checking and proving whether the distance z is in the far field by examining the inhomogeneity of the surface along the chosen frequency.

The volumetric distribution of the field over the aperture for distance $z = 0.25\boldsymbol{R}, \boldsymbol{f} = 5$ GHz is shown in Fig. 9. From the figure we can see the difference between amplitudes during point shift along the X and Y axes. This figure proves that higher difference between fields exists near the central aperture axis (small $\boldsymbol{r_0}$). Points of best visible difference are shown in arrows. This difference reaches 20% of the normalized field maximum. The lower distance $z = 0.25\boldsymbol{R}$ was taken for better visibility and due to the fact, that inequality also rises closer to the aperture.

IV. COMPARISON WITH GTD AND PWS

Fig. 10, 11 show the near-field calculations given in [5] for a circular aperture. Note that in Figures 10 and 11 the IRFs are considered as the benchmark. In Fig. 10, the distance from the observation point to the aperture plane is $z = 10\boldsymbol{\lambda}$, and the aperture diameter $\boldsymbol{d} = 2\boldsymbol{R} = 10\boldsymbol{\lambda}$. In Fig. 11, the distance from the observation point to the aperture plane is $z = 1000\boldsymbol{\lambda}$,

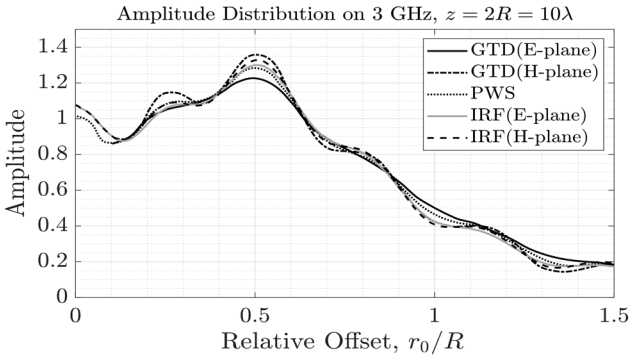

FIGURE 11. The near-field calculation results for a circular aperture. Distance to the aperture plane z = 1000λ (diameter D = 100λ).

and the aperture diameter $\boldsymbol{d} = 2\boldsymbol{R} = 100\boldsymbol{\lambda}$. The GTD results were reconstructed from [12] and [13]. As shown in Fig. 10, 11 the results are extremely close. In Fig. 10, the results of the PIRF calculations are located between those obtained using the GTD and PWS. As shown in Fig. 11, these values are slightly higher than those obtained with PWS.

We believe that the discrepancy is due to the lack of accuracy of the PWS method, as it is considered to be a near-field calculation with the decomposition of plane waves. The E-plane and H-plane PIRF results in Fig. 11 match exactly because the Z coordinate is in the far field.

V. CONCLUSION

This paper focuses on the features of the field distribution using the IRF method, and a more detailed comparison with the methods of calculating (FIT, GTD, PWS) is beyond its scope. Paper describes a detailed analysis of the linearly polarized EM field from the aperture antenna and how its characteristics change depending on the observation point. The difference between the primitive impulse response, which describes the field intensity at the same offset along the X- and Y-axes, reaches a significant value. In some cases, this should be considered when calculating antenna parameters.

The results showed that the PIRF method was much more effective in terms of computer resources than the GTD and PWS methods.

In the case of the PIRF, the obtained expressions for the field allowed us to more accurately calculate the flat aperture field in large regions of space, where all known calculation methods (finite integration technique, method of moments, GTD, and PWS) became too difficult to implement (finite integration technique, method of moments) or did not provide the necessary accuracy (PWS). As the observation point moves away from the aperture, the impulse response duration decreases; therefore, it is important to choose the proper time window so that the full impulse falls within it and to choose the number of points on the impulse needed to ensure a given accuracy after the Fourier transform.

The PIRF method is very convenient for calculating the fields of circular or rectangular apertures with a constant field

distribution over the aperture [19], [20] and with decreasing distributions of the form $g(r_o) = \left(1 - r_0/R^2\right)^n$, where R is the aperture radius and r_0 is the distance from the aperture center to the aperture point [21]. The distribution $g(r_0)$ can be represented as the sum of different distributions.

Finally, the PIRF method can be used for direct measurement of the antenna pattern with an aperture probe [22]. It was shown that the distance between antennas in direct measurements of the antenna pattern can be reduced by a factor of two (for the case of a linear, circular, or square antenna) compared to the generally accepted criterion of the far zone.

Comparing the PIRF method with GTD and PWS in the Fresnel zone and in the far field requires further research. We would be glad if specialists in GTD and PWS methods could get in touch with us.

REFERENCES

[1] R. Rudduck and C.-L. Chen, "New plane wave spectrum formulations for the near-fields of circular and strip apertures," *IEEE Trans. Antennas Propag.*, vol. AP-24, no. 4, pp. 438–449, Jul. 1976.

[2] R. C. Rudduck, D. C. F. Wu, and M. R. Intihar, "Near-field analysis by the plane-wave spectrum approach," *IEEE Trans. Antennas Propag.*, vol. AP-21, no. 2, pp. 231–234, Mar. 1973.

[3] H. G. Booker and P. C. Clemmow, "The concept of an angular spectrum of plane waves, and its relation to that of polar diagram and aperture distribution," *Proc. IEE-III, Radio Commun. Eng.*, vol. 97, pp. 11–17, Jan. 1950.

[4] J. Brown, "Theoretical analysis of some errors in aerial measurements," *Proc. IEE-C, Monographs*, vol. 105, pp. 343–351, Feb. 1958.

[5] R. Menendez, S. Lee, Y. Rahmat-Samji, and R. Rudduck, "Comments on 'new plane wave spectrum formulations for the near-fields of circular and strip apertures,"' *IEEE Trans. Antennas Propag.*, vol. AP-25, no. 6, pp. 908–912, Nov. 1977.

[6] A. Grebennikov, "Author's reply," *IEEE Trans. Microw. Theory Techn.*, vol. 63, no. 8, pp. 2705, Aug. 2015.

[7] R. Menendez, S. W. Lee, and Y. Rahmat-Samii, "New plane wave spectrum formulations for the near-fields of circular and strip apertures," *IEEE Trans. Antennas Propag.*, vol. AP-25, pp. 911–912, Nov. 1977.

[8] J. B. Keller, "Geometrical theory of diffraction," *J. Opt. Soc. Amer.*, vol. 52, no. 2, pp. 116–130, 1962.

[9] S.-W. Lee and G. Deschamps, "A uniform asymptotic theory of electromagnetic diffraction by a curved wedge," *IEEE Trans. Antennas Propag.*, vol. AP-24, no. 1, pp. 25–34, Jan. 1976.

[10] D. S. Ahluwalia, R. M. Lewis, and J. Boersma, "Uniform asymptotic theory of diffraction by a plane screen," *SIAM J. Appl. Math.*, vol. 16, no. 4, pp. 783–807, Jul. 1968.

[11] R. Menendez and S. W. Lee, "Uniform asymptotic theory applied to aperture diffraction," Dept. Elect. Eng., Univ. Illinois, Urbana, IL, USA, Tech. Rep., 76-3, 1974.

[12] R. G. Kouyoumjian and P. H. Pathak, "A uniform geometrical theory of diffraction for an edge in a perfect conducting screen," *Proc. IEEE*, vol. 62, no. 11, pp. 1448–1461, Nov. 1974.

[13] P. A. J. Ratnasiri, R. G. Kouyoumjian, and P. H. Pathak, "The wide angle side lobes of reflector antennas," Ohio State Univ., Columbus, OH, USA, Tech. Rep., 2183-1, Mar. 1970.

[14] S. P. Skullcin and V. I. Turchin, "Transient field calculation of aperture antennas," *IEEE Trans. Antennas Propag.*, vol. 47, no. 5, pp. 929–932, May 1999.

[15] S. P. Skulkin, N. A. Lysenko, G. K. Uskov, and A. M. Bobreshov, "Formulas for antenna patterns in time domain and for the primitive impulse response function of linearly polarized field of plane aperture," *IEEE Antennas Wireless Propag. Lett.*, vol. 19, no. 9, pp. 1516–1520, Sep. 2020, doi: 10.1109/LAWP.2020.3008116.

[16] N. A. Lysenko, S. P. Skulkin, E. Kopytin, and G. K. Uskov, "Primitive impulse response function for near-field calculation and its accuracy," *IEEE Antennas Wireless Propag. Lett.*, vol. 20, no. 12, pp. 2265–2269, Dec. 2021, doi: 10.1109/LAWP.2021.3106567.

[17] N. A. Lysenko, G. K. Uskov, A. M. Bobreshov, and S. P. Skulkin, "Limitations of aperture antenna theory for accurate transient field calculation in the time domain," in *Proc. IEEE Int. Symp. Antennas Propag. North Amer. Radio Sci. Meeting*, Montreal, QC, Canada, Jul. 2020, pp. 1057–1058, doi: 10.1109/IEEECONF35879.2020.9329917.

[18] S. P. Skulkin, "Near-field scanning in the time domain," in *Proc. Int. Symp. Antennas*, Nice, France, Nov. 1996, pp. 321–327.

[19] S. P. Skulkin, "Transient fields of rectangular aperture antennas," in *Ultra-Wideband, Short-Pulse Electromagnetics*, vol. 3. New York, NY, USA: Plenum, 1997, pp. 81–87.

[20] N. A. Lysenko, S. P. Skulkin, G. K. Uskov, K. V. Smuseva, and A. A. Potapov, "Applying a novel analytical method of calculation EM field to rectangular aperture and confirmation of the results by numerical modelling," in *Proc. IEEE Conf. Antenna Meas. Appl. (CAMA)*, Dec. 2022, pp. 14–17, doi: 10.1109/CAMA56352.2022.10002502.

[21] S. P. Skulkin, V. I. Turchin, N. I. Kascheev, and D. M. Ponomarev, "Transient field calculation of aperture antennas for various field distributions over the aperture," *IEEE Antennas Wireless Propag. Lett.*, vol. 16, pp. 2295–2298, 2017, doi: 10.1109/LAWP.2017.2715323.

[22] S. P. Skulkin, V. I. Turchin, and N. I. Kascheev, "Range distance requirements for large antenna measurements for square aperture with uniform field distribution," *IEEE Antennas Wireless Propag. Lett.*, vol. 17, no. 7, pp. 1257–1260, Jul. 2018, doi: 10.1109/LAWP.2018.2841645.

SERGEY P. SKULKIN was born in Gorky (now Nizhny Novgorod), Russia, in 1961. He received the M.Sc. degree from State Technical University, in 1983, and the Ph.D. degree in radiophysics from the Radiophysical Institute, Nizhny Novgorod, in 1995.

Since 1983, he has been an Engineer, a Research Scientist, and a Senior Research Scientist with the Radiophysical Institute. From 1987 to 1993, he was an Associate Professor with Nizhny Novgorod State Technical University. Since 2014, he has been a Professor with the Faculty of Business Informatics and Applied Mathematics, National Research University Higher School of Economics, Nizhniy Novgorod. His research interests include microwave and time-domain imaging, transient fields of aperture antennas, and antenna measurements.

Dr. Skulkin received the 1994 and 1995 URSI Young Scientists Award and the 1995 Swiss Academy of Engineering Science (SATW) Fellowship. In 1995, the U.S. Air Force sponsored his lectures and seminars with NIST, Boulder, CO, USA, the Rome Laboratory, Lexington AFB, MA, USA, and the Philips Laboratory, Kirtland AFB, NM, USA. Since 2018, he has been a delegate from Russia and Belarus to the European Association for Antennas and Propagation (EurAAP) (https://www.euraap.org/who-we-are). From 2017 to 2020, he was a Reviewer of IEEE TRANSACTIONS ON ANTENNAS AND PROPAGATION. In 2020, he was a Reviewer of IEEE ACCESS.

GRIGORY K. USKOV (Member, IEEE) was born in Voronezh, Russia, in 1980. He received the Ph.D. degree in radiophysics, in 2006, and the Doctor of Physics-Mathematics degree in radiophysics, in 2013. He was an Associate Professor with the Electronic Department, Voronezh State University. In 2020, he was a Professor with Voronezh State University, where he is currently the Head of the Electronic Department. His main research interests include UWB antennas, ultrashort pulse generators, metamaterials and dielectric structures, electromagnetic compatibilities, nonlinear effects in microwave active devices, and massive MIMO.

NIKOLAY A. LYSENKO was born in Voronezh, Russia, in 1992. He received the B.S. and M.S. degrees in radiophysics and the Ph.D. degree in electromagnetic propagation and antennas from Voronezh State University, in 2015 and 2019.

From 2014 to 2020, he was an Electronics Engineer. From 2015 to 2019, he was an Assistant Professor with the Electronics Department, Voronezh State University. Since 2020, he has been a leading Engineer with the Mathematical Modeling Department at a start-up in Yerevan, (remote work); and since 2021 he has been a Senior Researcher with the Electronics Department in Voronezh State University. He is the author of one student book, and more than 12 articles. He is a reviewer of Microwave and Optical Technology Letters, and holds two patents. He participated in more than 15 grants and projects.

His research interests include ultra-wideband (UWB) and aperture antennas, 5G antenna arrays, MIMO beamforming, analytical and numerical time domain (TD) electromagnetic (EM) field analysis non-uniform dielectric materials and lenses. Also he has been working on remote surface sensing, radio-imaging technology, TX/RX path.

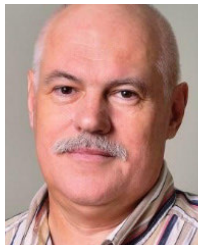

NIKOLAY I. KASCHEEV was born in Gorky (now Nizhny Novgorod), Russia, in 1958. He received the M.Sc. degree from State Technical University, in 1980, and the Ph.D. degree from Nizhny Novgorod State Technical University, Nizhny Novgorod, in 1991.

Since 2014, he has been the Head of the Basic Chair, MERA, Faculty of Business Informatics and Applied Mathematics, National Research University Higher School of Economics, Nizhniy Novgorod. Since 2014, he has been the Director of the Nizhny Novgorod Information Technology Institute. He performs research in the sphere of modern information technologies. He is the author of more than 80 research articles and publications. His research interests include developing methods and algorithms to test digital gadgets, imitation modeling, and the creation of non-invasive glucometers.